Developmental Cognitive Neuroscience 35 (2019) 94–103

Contents lists available at ScienceDirect

Developmental Cognitive Neuroscience

journal homepage: www.elsevier.com/locate/dcn

Processing of affective and emotionally neutral tactile stimuli in the insular cortex

Monika Davidovic[a,*], Göran Starck[b,c], Håkan Olausson[a,d]

[a] Institute of Neuroscience and Physiology, University of Gothenburg, Gothenburg, Sweden
[b] Department of Radiation Physics at the Institute of Clinical Sciences, University of Gothenburg, Gothenburg, Sweden
[c] Department of Medical Physics and Biomedical Engineering, Sahlgrenska University Hospital, Gothenburg, Sweden
[d] Center for Social and Affective Neuroscience (CSAN), Linköping University, Linköping, Sweden

ARTICLE INFO

Keywords:
Touch
fMRI
Insula
Resting state networks

ABSTRACT

The insula is important for the processing of pleasant aspects of touch whereas its role in the processing of emotionally neutral touch has been less explored. Here, we used a network approach to investigate the insular processing of pleasant stroking touch and emotionally neutral vibratory touch, analysing functional magnetic resonance imaging data from 23 healthy adult participants. Vibration and skin stroking activated areas in the posterior, middle and anterior insula. Psychophysiological interaction analyses suggested that skin stroking increased functional connectivity between the posterior and ventral anterior insula. Vibration instead increased functional connectivity between the posterior and dorsal anterior insula, and induced a stronger decrease of the default mode network activity compared to stroking. These results confirmed findings from previous studies showing that the posterior insula processes affective touch information. We suggest that this is accomplished by relaying tactile information from the posterior insula to ventral anterior insula, an area tightly connected to the emotional parts of the brain. However, our results also suggested that the insula processes tactile information with less emotional valence. A central hub in this processing seemed to be the right dorsal anterior insula.

1. Introduction

A plethora of animal and human experimental studies, and clinical observations, show a critical role for touch in brain development and attachment (Barnett, 2005). Already in utero the tactile receptors of the skin are stimulated by movements of the amniotic fluid, a mechanism which is speculated to be important for fetal growth (Bystrova, 2009). In newborns, tactile interactions, besides visual, auditory, and olfactory stimulations, are important for the development of social bonds, and gentle caressing can constitute up to 30% of the time mothers interact with their newborns (Stack and Muir, 1992). Slowly stroking touch in infants decreases heart rate suggesting an increased activity of the parasympathetic nervous system (Fairhurst et al., 2014). In pre-school children the frequency of maternal touch, as measured in a play session, positively correlates to activity in social brain networks (Brauer et al., 2016). During adolescence touch remains important for our physical and psychological well-being (Sehlstedt et al., 2016). Furthermore, in adults reduced valence ratings of touch is associated with childhood maltreatment (Croy et al., 2016). The importance of tactile stimulation for early brain development suggests an important role for touch in neurodevelopmental disorders. Consequently, many psychiatric conditions are associated with touch avoidance (Cascio, 2016) and children with autism spectrum disorder generally perceive touch as being less pleasant than typically developing children (Cascio et al., 2016).

Gentle stroking of the hairy skin activates two groups of afferents: myelinated Aβ and unmyelinated C-tactile or CT afferents. Microneurography studies of spike trains in peripheral afferents induced by skin stroking at different velocities show that both Aβ and CT afferents are velocity sensitive (Ackerley et al., 2014; Löken et al., 2009). However, while the mean firing frequency of Aβ afferents increases with increasing velocity of the skin stroking, CT afferents show a parabolic dependence with the maximum mean firing frequencies at

Abbreviations: CT, C tactile; IC, insular cortex; pIC, posterior insular cortex; LpIC, left posterior insular cortex; aIC, anterior insular cortex; daIC, dorsal anterior insular cortex; vaIC, ventral anterior insular cortex; RdaIC, right dorsal anterior insular cortex; vmPFC, ventro medial prefrontal cortex; daCC, dorsal anterior cingulate cortex; pCC, posterior cingulate cortex; pgaCC, pregenual anterior cingulate cortex; mTG, medial temporal gyrus; lfrs, low frequency resting state; DMN, default mode network; SN, salience network; CEN, central executive network; VAS, visual analogue scale; BOLD, blood oxygenation level dependent; MRI, magnetic resonance imaging; GM, grey matter; MNI, Montreal Neurological Institute; GLM, general linear model; PPI, psychophysiological interaction; FEW, family-wise error; ROI, region of interest

* Corresponding author at: Blå Stråket 7, 41345 Gothenburg, Sweden.
E-mail address: monika.davidovic@neuro.gu.se (M. Davidovic).

https://doi.org/10.1016/j.dcn.2017.12.006
Received 28 February 2017; Received in revised form 15 November 2017; Accepted 19 December 2017
Available online 22 December 2017
1878-9293/ © 2017 The Authors. Published by Elsevier Ltd. This is an open access article under the CC BY-NC-ND license (http://creativecommons.org/licenses/BY-NC-ND/4.0/).

the velocities 1–10 cm/s. Psychophysiological experiments of gentle skin stroking show that the perceived pleasantness at the different velocities of skin stroking follows a similar parabolic curve as mean firing frequency of CT afferents (Löken et al., 2009). Therefore, it has been proposed that an important role of CT afferents is to contribute to the emotional experience of touch. In this context, the Aβ tactile input is described as having discriminative properties (such as to detect and identify stimuli) while the CT input underpins affective functions of tactile sensations (Olausson et al., 2010; McGlone et al., 2014). In addition, it has been shown that the velocity preference for stroking in the range of 1–10 cm/s is present already in the early childhood (Croy et al., 2017) and is persistent throughout life (Sehlstedt et al., 2016). Furthermore, it has been suggested that CT afferents present a preserved evolutionary system involved in the rewarding value of physical contact in nurturing and social interactions (McGlone et al., 2014).

Brain imaging studies on two subjects lacking Aβ afferents show that isolated activation of CT afferents with light skin stroking leads to an increased blood oxygenation level dependent (BOLD) signal in the contralateral posterior insular cortex (*pIC*) (Olausson et al., 2002; Olausson et al., 2008). In addition, no activation is observed in the postcentral gyrus or parietal operculum, suggesting that the *pIC* might be the primary brain area for CT input. Several additional studies point in the same direction (Morrison et al., 2011a, 2011b; Björnsdotter et al., 2009) and establish the notion of an anatomically distinct affective touch pathway, which includes CT afferents in the periphery and with *pIC* as a target area for brain processing. The discriminatory touch pathway, on the other hand, comprises Aβ afferents in the periphery and with the primary and secondary somatosensory cortices (*S1* and *S2*) as target areas for brain processing (Olausson et al., 2010; McGlone et al., 2014).

Anatomically, the CT afferent pathway shares similarities with temperature and pain projections, and in extension with all unmyelinated afferents that take the lamina I pathway in the spinal cord, and which are associated with the process of interoception. In this view, the input from CT afferents is not only important for the positive, hedonic experience of the touch, but also contributes to the sense of the physiological condition of the body and wellbeing (Craig, 2002). It is proposed that the insular processing of the input from bodily unmyelinated afferents proceeds through a series of re-representations of the neuronal information, which starts in the *pIC* and goes via the middle insula to the anterior insular cortex (*aIC*). Posterior-middle-anterior progression is accompanied by the higher-level integration of information from other sensory modalities and results in the unified percept of subjective awareness (Craig, 2002).

The insula is anatomically divided by a central insular sulcus into a posterior and an anterior part. The posterior insula is composed of two long gyri while the anterior insula has between 3 and 5 gyri. All insular gyri extend in the dorsal-ventral direction where they join together in a hub at the ventral basis of the insula. Histological investigations of the insular cortex show changes in the second and fourth granular layers with the ventral insula being agranular and dorsal insula being dysgranular-granular (Mesulam and Mufson, 1982; Kurth et al., 2010a; Morel et al., 2013). Agranular and granular parts of the insula have different neurodevelopmental trajectories (Shaw et al., 2008): while the ventral anterior insular cortex (*vaIC*) follows a linear growth trajectory with monotonically decreasing cortical thickness both during childhood and adolescence, the granular cortex of the *pIC* and the dorsal part of anterior insular cortex *(daIC)* follow a more complex cubic trajectory with increasing cortical thickness during childhood and decreasing cortical thickness during adolescence.

Several meta-analyses (Kurth et al., 2010b; Uddin et al., 2014) show that the functional differentiation of the insula follows the anatomical and the histological ones. A threefold functional partition of the insula is proposed: sensory *pIC*, cognitive *daIC* and affective *vaIC* (Fig. 1). The additional role of *daIC* emerged from the studies on low frequency resting state networks (*lfrs-networks*): the salience network (SN), the default mode network (DMN) and the central executive network (CEN). The *daIC*, together with the dorsal part of anterior cingulate cortex *(daCC)*, belongs to the SN (Uddin, 2015), and it is suggested that the function of the SN, and the right *daIC* (*RdaIC*) in particular, is to switch between the DMN and CEN (Uddin, 2015).

The DMN consists of a set of brain areas located in the ventral medial prefrontal cortex (*vmPFC*), posterior cingulate cortex (*pCC*) and bilateral lateral posterior parietal cortices (Raichle, 2015). It is characterized by high functional connectivity in resting state functional magnetic resonance imaging (fMRI) experiments, and decreased activity level during task fMRI experiments. In addition, it is observed that the DMN and CEN are anti-correlated in resting state experiments. A decrease in the DMN during cognitive tasks depends on the task difficulty and is most pronounced in attention-demanding, non-self-referential tasks. The decrease in the DMN and increase in the CEN during task performance is one example of the network organization of brain activity that maintains energy consumption balance. On the other hand, high activity in DMN hubs, especially in the *vmPFC*, is associated with emotional processing of sensory information (Raichle, 2015; Dosenbach et al., 2007; Fox and Raichle, 2007).

Recently, we investigated brain responses to two types of tactile stimuli with fMRI: light skin stroking at 2 cm/s and static vibration (Davidovic et al., 2016). Skin stroking was perceived as pleasant by the participants, while vibration produced an emotionally neutral percept. These two tactile stimuli have different effects on the Aβ and CT afferents. Importantly, while skin stroking at 2 cm/s is an optimal CT stimulus, vibration is a poor CT stimulus (Olausson et al., 2002). On the other hand, both 2 cm/s skin stroking and vibration are effective for activating Aβ afferents. Contrary to what we predicted, we found that both types of tactile stimuli, i.e. both discriminative and affective touch resulted in an increase in the BOLD signal in the posterior, middle and anterior insula (Davidovic et al., 2016).

To better understand these processes, we performed a detailed investigation of the effects of stroking and vibration on the insula, and in addition on the DMN, using data from a previous study (Davidovic et al., 2016). We specifically tested the hypothesis that both affective and discriminative stimuli are functionally processed in the insula. We predicted that affective (stroking) touch involves functional processing in the emotional *vaIC*, and also in hubs of the DMN. Furthermore, discriminatory (vibratory) touch should have a stronger impact on the DMN, partially through the *RdaIC* switch (the central hub in the SN). We also hypothesized that the information about discriminatory and affective touch is processed in the insula through different pathways. Since vibration and skin stroking differ in both Aβ and CT input, investigating psychophysiological interaction (PPI) is better suited to studying higher level processing than the method of pure insertion (Friston et al., 1996). Considering that information processing in the insula is suggested to follow posterior-middle-anterior progression, we performed a functional connectivity analysis within the insula, with seeds placed in the putative primary receiving area for CT input (*LpIC*; contralateral to the side of stimulation) and the switch between the DMN and CEN (*RdaIC*).

2. Materials and methods

2.1. Participants

Twenty-three healthy subjects participated in the study (11 males, mean age 25 years, range 19–38 years). All subjects were right-handed as assessed through the Edinburgh Handedness Inventory. Ethical approval was obtained by the ethics board of Gothenburg University (Dnr: 890-13). Participants were compensated with 200 Swedish crowns (approximately 20 Euro) per hour.

2.2. Experimental protocol and stimuli

Each subject completed one resting-state, one anatomical (T1-

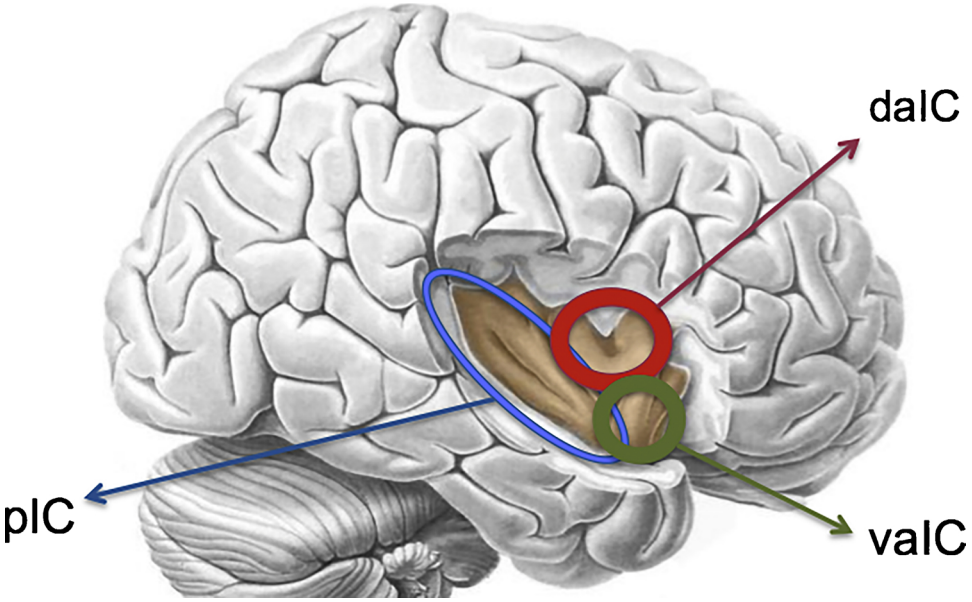

Fig. 1. Functional differentiation of insula: sensory (posterior insular cortex; pIC), emotional (ventral anterior insular cortex; vaIC) and cognitive (dorsal anterior insular cortex; daIC).

weighted) and one task session (in this order). During the resting state session, which lasted 10 min, subjects were instructed to keep their eyes closed, think of nothing in particular, and not to fall asleep.

A detailed description of the task session is provided in a previous paper (Davidovic et al., 2016). The experimenter applied tactile stimuli by hand. Gentle skin stroking was applied by a 6-cm wide artist's brush at a speed of 2 cm/s across a distance of 10 cm, in a proximal to distal direction. Vibration (100 Hz) was delivered with a device consisting of a rectangular piece (40 × 12 × 7 mm) of balsa wood connected to a piezo-element. The area of skin that was stimulated by vibration was 480 mm^2. Both stimuli were applied on the right anterolateral surface of the thigh. Each tactile stimulus lasted for 15 s. One block contained one stroking stimulus (15 s), one vibration stimulus (15 s) and a behavioral assessment (15 s). In the behavioral assessment, participants were asked to rate the perceived pleasantness of the last stimulus on a visual analogue scale (VAS). The cursor on the VAS scale was initially placed at the center marked 'neutral', and the endpoints of the VAS were 'unpleasant' and 'pleasant'. The scale was subsequently converted to the range −5 to 5 for the statistical assessment. The scanning session comprised one run with 12 blocks, each block separated by a 15 s rest period.

2.3. MRI acquisition

MRI was performed on a Philips Gyroscan 3T Achieva, software release 3.2, (Philips, Eindhoven, The Netherlands). A T1-weighted scan (3D T1-TFE) with scan resolution 1.0 × 1.0 × 1.0 mm^3 was performed as anatomical reference. Functional resting state data comprised 200 and task data 245 volume images of the brain (parameters: single shot gradient echo, echo planar imaging with flip angle 90°, TE = 35 ms, TR = 3000 ms, SENSE factor 1.8, 40 axial slices without slice gap and with scan resolution 2.8 × 2.8 × 2.8 mm^3).

2.4. fMRI data preprocessing

Preprocessing and statistical analysis of anatomical and functional (both the resting state and task session) images were performed using SPM8 (http://www.fil.ion.ucl.acuk/spm). The anatomical images were segmented into grey matter (GM), white matter and cerebrospinal fluid images. The GM images were used to determine the 12-parameter affine transformation onto the standard stereotactic space (Montreal Neurological Institute, MNI). Functional data preprocessing included slice time correction, realignment to the first volume of the first run (using a 6-degree rigid spatial transform), co-registration to anatomical images, transformation to MNI space (using the 12 parameters obtained from transformation of GM images), resampling to voxels 2 × 2 × 2 mm^3 and smoothing with a 6-mm full width at half maximum Gaussian kernel. In addition, motion artefacts were examined using the Artefact Detection Toolbox (http://www.nitrc.org/projects/artifact_detect/). Volumes in which the global signal deviated more than two standard deviations from the mean signal or in which the difference in motion between two neighboring volumes exceeded 1 mm (across rotational or translation directions) were marked as outlier volumes. Smoothed functional images were filtered with a 128 s high pass filter.

2.5. Analysis of resting state data

The purpose of this analysis was to identify two *lfrs-networks*: DMN and SN. These networks were identified with a seed to voxel analysis, using the Functional Connectivity (CONN) toolbox v15 (Whitfield-Gabrieli and Nieto-Castanon, 2012), implemented in SPM8.

Preprocessed data were band pass filtered at 0.008–0.09 Hz. Two different seeds in the form of spheres with radius 10 mm were used. For the construction of the DMN, the center of the sphere was placed in the *pCC* (MNI coordinate 0, −56, 28), and for the construction of the SN the sphere was placed in the *daCC* (MNI coordinate 0,6,40). Both seeds are predefined in CONN toolbox. The seed driven analysis was performed by calculating the Pearson's correlation coefficients between the seed's time course and the time course of all other voxels. The correlation coefficients were then converted to normally distributed scores using Fisher's transform, and passed to a second-level general linear model (GLM) analysis. The resulting whole brain maps were thresholded at $p < .001$ (FWE corrected).

2.6. Group level analysis of task data

We defined four regressors (stroking, vibration, VAS rating for stroking, VAS rating for vibration) using a boxcar function with 1 during the 15 s stimulus and rating conditions and 0 otherwise, convolved with the canonical hemodynamic response function. The design matrix also included motion parameters (3 rotational and 3 translational) and outlier volumes as regressors of no interest. Detailed information about the number and distribution of outliers is presented in

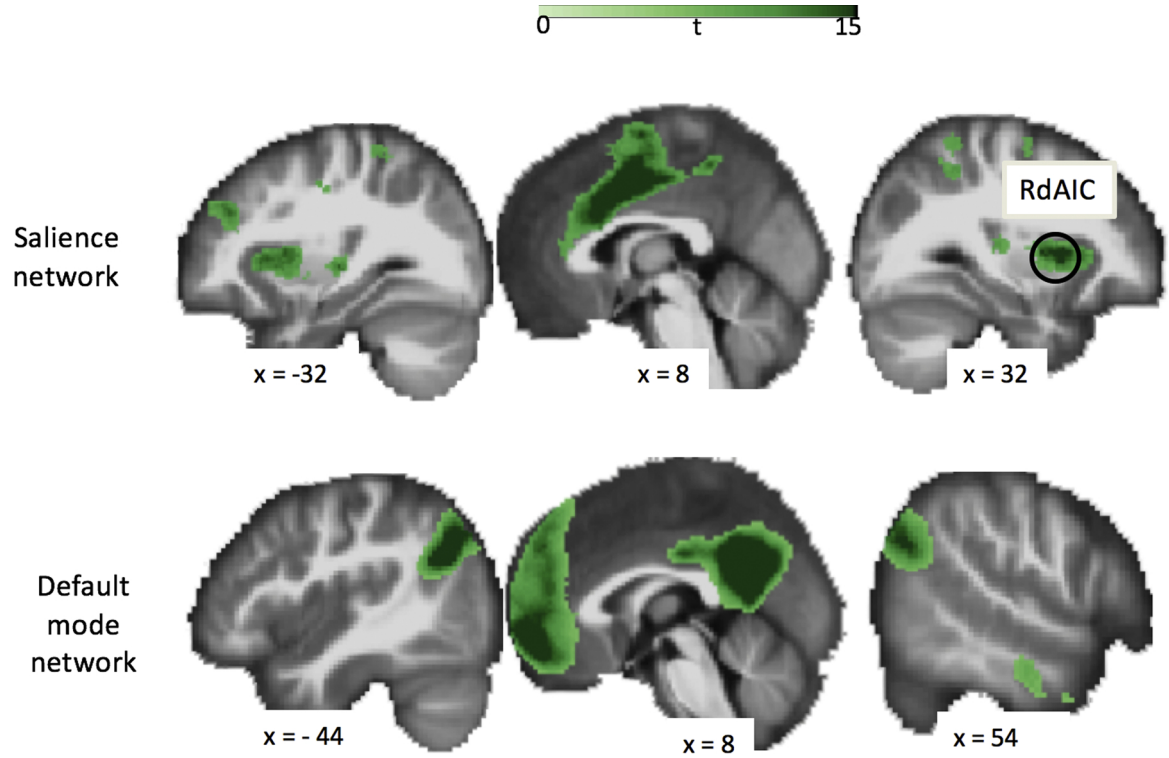

Fig. 2. Results from the resting state seed-to-voxel analysis, low frequency resting state networks. Salience network: black circle highlights the location of the peak in the right dorsal anterior insular cortex (RdaIC). Default mode network: green areas correspond to the DMN mask. Both maps are thresholded at FWE corrected $p < .001$.

a previous paper (Davidovic et al., 2016). Parameter estimates (beta values) of BOLD responses were calculated for both tactile conditions (stroking and vibration) and for the difference between conditions. These were passed to the second level mixed effect group analysis.

2.7. Definition of masks and regions of interest

We defined two masks and three regions of interest (ROIs), which we used in the analysis of task data:

1. Bilateral *insular cortex mask*: from Harvard-Oxford Structural Atlas (http://www.cma.mgh.harvard.edu/fsl_atlas.html).
2. Default mode network *DMN mask*: obtained by thresholding the map from resting state data, seed-to-voxel analysis, with seed in the *pCC* (as described in Section 2.5.) (Fig. 2).
3. *RdaIC ROI*: sphere with radius 10 mm, centered at the peak value in *RdaIC* in the SN map. SN was obtained by thresholding the map from the resting state seed-to-voxel analysis with seed in the *daCC* (as described in Section 2.5.) (Fig. 2).
4. *LpIC ROI*: sphere with radius 10 mm, centered at the peak with MNI coordinates: −38, −16, 6. This was guided by the work of Björnsdotter et al. (Björnsdotter et al., 2009), where multivariate voxel clustering analysis was used to estimate the peak coordinates in the *LpIC*, for the skin stroking stimulus on the right arm and right thigh, in six healthy subjects. Here, we used the six coordinates reported for the skin stroking on the right thigh and by addition and subtraction found the center for the *LpIC*ROI.
5. *LS1 ROI*: sphere with radius 10 mm, centered at MNI coordinates −24, −42, 62 for stroking and −22, −40, 68 for vibration, as reported in a previous study (Davidovic et al., 2016).

2.8. Task data analyses within predefined masks and ROIs

We start by presenting the data for the main effect of stroking and vibration, within the bilateral insular cortex mask. Although these results have already been presented in a previous paper at the whole brain level (Davidovic et al., 2016), we show them here in sagittal slices since these images give a better appreciation of the pattern of activation in the insula for the stroking and vibration. This is important for the later discussion in section 4.

Next, we present analysis for the contrast stroking > vibration within the DMN mask, thresholded at $p < .005$ and corrected for multiple comparison at $\alpha < 0.05$, which corresponds to the cluster size > 24 voxels, as assessed through Monte Carlo simulations implemented in Matlab (Song et al., 2011). The purpose of this analysis is to establish the levels of activity in the DMN during the stroking and vibration.

To perform detailed comparison of activations in the primary somatosensory areas with activations in the DMN areas, we also extracted average beta values for both stroking and vibration using MarsBar toolbox (http://marsbar.sourceforge.net/) for the *LS1* and *LpIC* ROIs, as defined in section 2.7, and for the 10 mm spheres at peak coordinates for the contrast stroking > vibration, within the DMN mask. The purpose of this analysis is to establish whether the alterations in the activity levels in the DMN are a consequence of the difference in the amount of the primary somatosensory input (bottom up input) or reflect the processing of information at the higher levels. We also extracted average beta values for the stroking and vibration in the *RdaIC* ROI, which we will use in the discussion in section 4.

2.9. Functional connectivity analysis

We performed two separate PPI analyses (Friston et al., 1997) as implemented in SPM8: one with the seed in the *RdaIC* ROI and one with the seed in the *LpIC* ROI. The purpose of these analyses is to investigate the pathways of processing of information related to the affective and discriminative touch. In the first step, a preprocessed BOLD signal was extracted from the seed region. In the second step, a PPI regressor was formed from the interaction between the extracted BOLD signal and the difference between the task regressors (stroking and vibration)

convolved with the canonical hemodynamic response function. In the third step, a GLM analysis was performed with the PPI regressor, task regressors, and the extracted BOLD signal. The motion parameters (3 rotational and 3 translational) and outliers were also included as regressors of no interest. The main effect for the PPI regressor for each subject was estimated. At the second level, random effect analysis was used to determine group effects. This resulted in a map that was thresholded within the bilateral insular cortex mask. The threshold was set at $p < .005$ and cluster size > 18 voxels, corresponding to the threshold of $\alpha < .05$ corrected for multiple comparison as assessed through Monte Carlo simulations implemented in Matlab (Song et al., 2011).

2.10. Conjunction analysis

We assessed overlap between the *RdaIC* and *LpIC* ROI functional connectivity maps by computing conjunction analysis, using the minimum statistic approach (Friston et al., 1999, 2005). This analysis allows us to test the hypothesis about the posterior-middle-anterior mechanism for the processing of the tactile information in the insula. We computed a 2-way conjunction between the PPI maps for seeds in the *RdaIC* and *LpIC*. Thresholding each map at $p < .01$ from this conjunction corresponds to a combined threshold of.001, uncorrected. Within the bilateral insular mask the clusters size of 9 voxels corresponds to a corrected threshold of $\alpha < .05$, as assessed with Monte Carlo simulations for this conjunction analysis.

3. Results

3.1. Lfrs-networks

Seed-to-voxel analysis with a seed placed in the *daCC* resulted in a map that comprised, among other areas, bilateral anterior insula (Fig. 2), corresponding to the SN (Uddin, 2015). From this map we identified the peak in the *RdaIC* at MNI coordinate 34, 12, 4, and constructed the *RdaIC* ROI (see Section 2.7).

Seed-to-voxel analysis with a seed placed in the *pCC* resulted in a map that comprised the *vmPFC*, bilateral ventral temporal lobe, and bilateral posterior parietal/temporal lobes, all parts of the DMN (Fig. 2) (Raichle, 2015). This thresholded map was used as the DMN mask (see Section 2.7).

3.2. Behavioral ratings of stimuli in the task experiment

Details about pleasantness ratings of tactile stimuli are presented in a previous paper (Davidovic et al., 2016). In summary, participants rated skin stroking as pleasant (mean 1.9; SD 1.1) and vibration as neutral (mean 0.4; SD 0.9). The difference in pleasantness ratings between stroking and vibration was significant (paired two-sample *t*-test $p < .001$).

3.3. Group analysis of task data

We first present the data for the main effect of stroking and vibration, within the bilateral insular cortex. As shown in Fig. 3, both stroking and vibration activated the posterior, middle and anterior parts of the left (contralateral side to the skin stroking) insula. In the right insula however, the pattern of activation differs between stroking and vibration: while stroking activates posterio-middle parts, vibration resulted in the activation increase in the anterior parts of the right insula.

When analysing stroking > vibration within the DMN mask we found significant differences in the *vmPFC*, *pCC* and bilateral posterior middle temporal gyrus (*RmTG* and *LmTG*) (Fig. 4, Table 1). We found no significant differences for the contrast vibration > stroking within the DMN mask. This suggests that the level of activity in the DMN is higher during stroking than during vibration.

Then, we investigated in detail the activation levels for stroking and vibration expressed as average beta values within a group of ROIs (Fig. 5). First we looked at the three predefined ROIs: *LS1*, *LpIC* and *RdaIC*. Both stroking and vibration resulted in significant activations in the *LS1* and *LpIC* (one-sample *t*-test $p < .001$ for both). The level of activation was higher for stroking than for vibration in both *LS1* (two sample *t*-test $p < .001$) and in *LpIC* (two sample *t*-test $p = .001$). In addition, both stroking and vibration activated the *RdaIC* (one-sample *t*-test gives $p = .004$ and $p = .005$ respectively). However, there was no difference in the level of activation in the *RdaIC* ROI for stroking and vibration ($p = .541$). After Bonferroni correction for three ROIs, the tests performed for the *S1* and *LpIC* were significant at the corrected value of $p < .01$.

Next, we investigated the levels of activity in the DMN for stroking and vibration (right side of Fig. 5). We found decreases in the levels of activation in the DMN for both stroking and vibration compared with the baseline (rest period). The significant positive t-values for contrast stroking > vibration within the DMN mask (Fig. 4) were a result of stronger deactivation for vibration than for stroking in the DMN. Note that the values in the DMN areas presented in Fig. 5 were extracted at the peak coordinates for the contrast stroking > vibration presented in Table 1 and Fig. 4. Thus, the purpose of presenting these values in Fig. 5 was to investigate the level of BOLD response in the DMN for stroking and vibration, not to test for the significant difference between them.

3.4. PPI analyses of task data

The results from the PPI analyses are presented in Fig. 6 and Table 2. Here, we can study differences in the patterns of functional connectivity between stroking and vibration, within the insula. For a seed in the *RdaIC* ROI, and for the contrast vibration > stroking, a significant cluster was observed in the right middle insula (Fig. 6A, Table 2). No significant clusters were observed for the contrast stroking > vibration. For a seed in the *LpIC* ROI, and for the contrast vibration > stroking, significant clusters were observed in the left middle insula and bilateral *daIC* (Fig. 6B, Table 2). For the contrast stroking > vibration we observed one cluster located in the left *vaIC* (Fig. 6B, Table 2).

3.5. Conjunction analysis

The results from the conjunction analysis for the PPI results with seeds in *RdaIC* and *LpIC* are presented in Fig. 6C and Table 2. We observed no overlapping areas for the contrast stroking > vibration. However, for the contrast vibration > stroking, two overlapping areas were found in the left and right middle insula.

4. Discussion

In this paper we investigated the insular processing of the discriminative and affective aspects of touch in adult healthy subjects. We performed extensive analyses of BOLD and functional connectivity responses to skin stroking and skin vibration in the insula. We hypothesized that the difference in the cognitive task evaluation between these two tactile stimuli will have an impact on the activity levels in the DMN, and that this effect is to some extent achieved through the processing of tactile information via the cognitive/discriminative pathways in the insula. Therefore, we extended the analyses also to the DMN.

Stroking and vibration were both effective in activating the insula. Although the level of activation in the *LS1* and *LpIC* was higher for stroking than for vibration, vibration decreased the levels of activation in the DMN more than stroking. Hence, the stronger decrease in the DMN for vibration is probably not a consequence of the intensity of the primary input, but the result of difference in the higher level processing. Vibration is an artificial type of touch that has low emotional

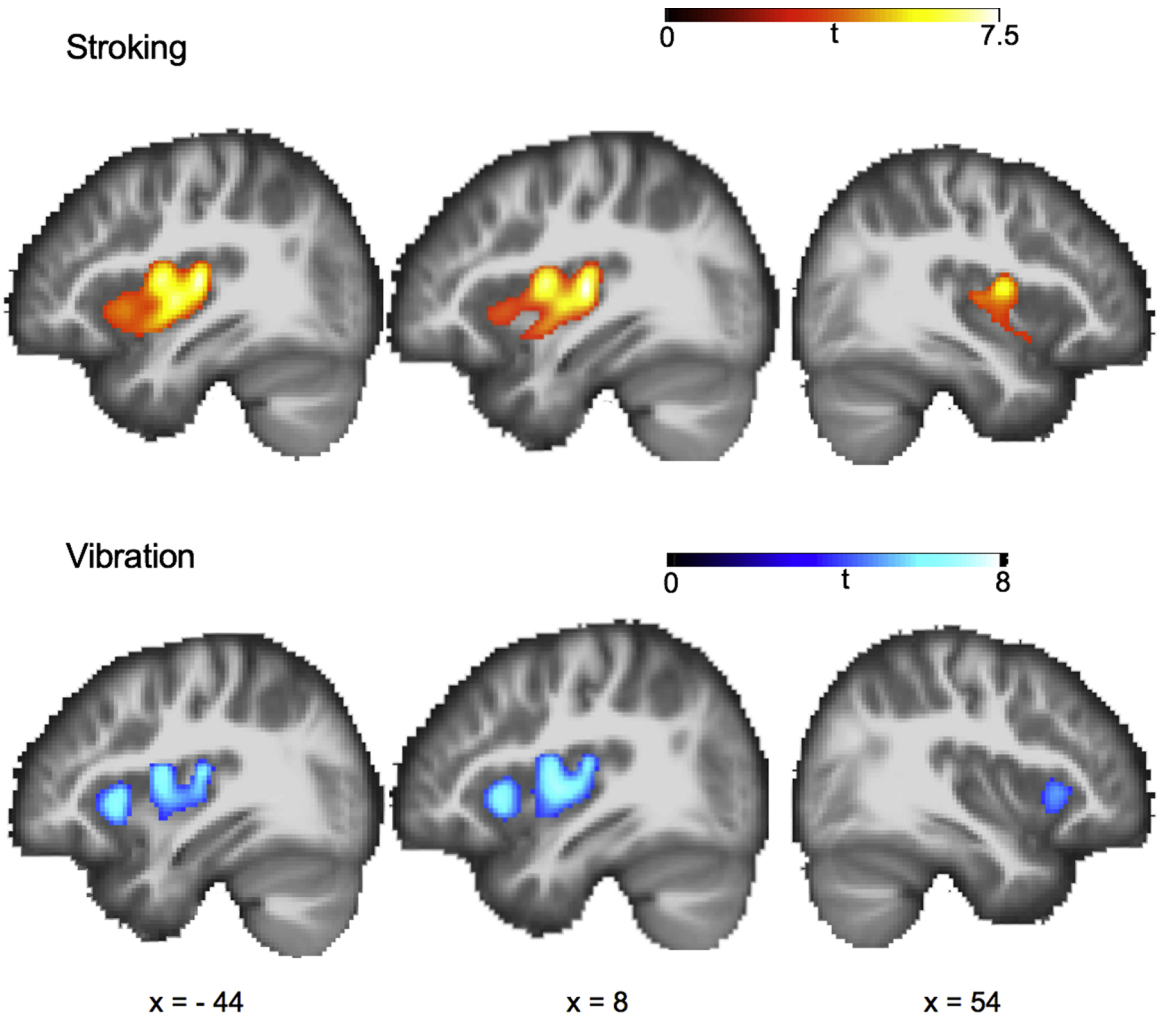

Fig. 3. Results from the task experiment, main effect for stroking and vibration (i.e. stimulus vs baseline), evaluated within bilateral insular mask and thresholded at $p < .001$.

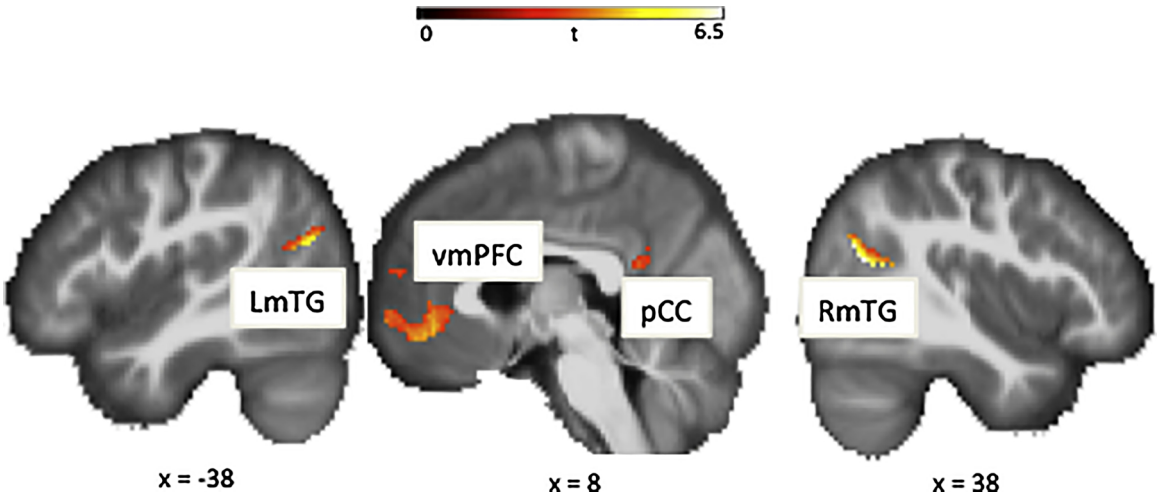

Fig. 4. Results from the task experiment, contrast stroking > vibration evaluated within the default mode network mask, thresholded at $p < .005$ and cluster size > 24. Abbreviations: left middle temporal gyrus (LmTG), ventro medial prefrontal cortex (vmPFC), posterior cingulate cortex (pCC), right middle temporal gyrus (RmTG).

valence. On the other hand, slow skin stroking is experienced in everyday life, e.g. during caresses, and is typically perceived as pleasant (Morrison et al., 2009). The task for the participants during both stimuli was to rate the pleasantness of the tactile stimulus.

Stroking was applied on a larger skin area than vibration. Thus, the number of peripheral afferents activated by stroking was likely larger than the number activated by vibration. This may explain the higher activity levels for stroking compared with vibration in the *S1*. Our results also showed a significant increase of activity in the *LpIC* for both stroking and vibration. Although the level of activity in the *LpIC* was smaller for vibration than for stroking, in light of the different activity levels in the *LS1*, we speculate that at least some part of this difference

Table 1
Results from the task experiment, contrast stroking > vibration: t-values, MNI coordinates and cluster sizes (ks). Map is masked with the default mode network (DMN) mask and thresholded at p < .005 and cluster size > 24. t-value of 3.5 corresponds to p = .001. *DMN coordinates at which beta values presented in Fig. 5 were extracted.

Region	t-value	x	y	z	ks
R Middle Temporal Gyrus*	6,5	42	−64	20	205
L Middle Temporal Gyrus*	5,3	−46	−70	22	106
L Posterior Cingulate Cortex*	4,8	−16	−52	20	367
R Posterior Cingulate Cortex	3,9	10	−52	18	367
L Ventro Medial Prefrontal Cortex*	4,8	−8	40	−6	441
L Ventro Medial Prefrontal Cortex	3,6	−4	64	−6	441
L Superior Medial Frontal Gyrus	4,3	−10	58	18	40
L Superior Medial Frontal Gyrus	4,2	−14	40	52	45

was due to the difference in the intensity of the input, and that isolated Aβ input suffices to activate the *pIC*.

All ROIs in this paper are spheres with the radius 10 mm. This size was guided by the sizes of predefined seeds in the CONN. Given this size, and the applied smoothing, with analyses presented in this paper we cannot say whether vibration and stroking activated the same parts of the *pIC* or have different areas for input in the *pIC*. The study on the somatotopic organization in the posterior insula suggests that CT afferents activated by stroking have their input in the *pIC* (Björnsdotter et al., 2009). Aβ afferents primarily activate the *S1* and *S2*, which in turn might activate the *pIC*. A study on a macaque monkey, in which single cell recordings were made during a skin stroking task shows that the *pIC* contains neurons that fire differently at different stroking velocities (Grandi and Gerbella, 2016). However, we note that the population of velocity sensitive neurons in the *pIC* found in that experiment consists of two types of neurons: those that respond with increased activity when velocity of stroking increases, and those that respond to velocities 1–5 cm/s but not to 5–15 cm/s. Compared with a microneurography study in humans (Löken et al., 2009), one possible interpretation of these results might be that the *pIC* contains neurons that selectively respond to the Aβ afferent input and neurons that selectively respond to the CT afferent input. Future studies with smaller voxel sizes are needed to resolve this question.

In addition to the *LpIC*, both stimuli also activated the *RdaIC*. This finding is in line with previous studies that show increases in BOLD response in the anterior insula during tactile perception tasks (Eck et al., 2013; Panchuelo et al., 2016; Perini et al., 2015). We also found that both *LpIC* and *RdaIC* displayed higher functional connectivity with the middle insula for the contrast vibration > stroking. In addition, conjunction analysis on the resulting maps from the PPI analyses indicated that the *LpIC* and *RdaIC* might communicate via the middle insula, and that this communication was more pronounced for discriminative touch than for affective touch. We note that, since stroking also resulted in an increased BOLD response in the *RdaIC*, it is probable that the same pathway *LpIC-RdaIC* is used in evaluation of stroking but to a smaller extent than for vibration.

A previous study of resting state functional connectivity of the insular cortex shows a functional partition in the anterior insula (Deen et al., 2011), where the *daIC* primarily connects to the *daCC*, which corresponds well to our identification of the *daCC-RdaIC* as the SN in our resting state results. In the same study, the *vaIC* displays functional connections notably to the pregenual anterior cingulate cortex *(pgaCC)*, an area important for the emotional processing of positively valenced (pleasant) sensory stimuli (Grabenhorst and Rolls, 2011; Grabenhorst et al., 2010). Subjective ratings of touch pleasantness correlate with BOLD signal in the *pgaCC* (Case et al., 2016), and the *pgaCC* is strongly activated by a human caress (Lindgren et al., 2012). In our study, the

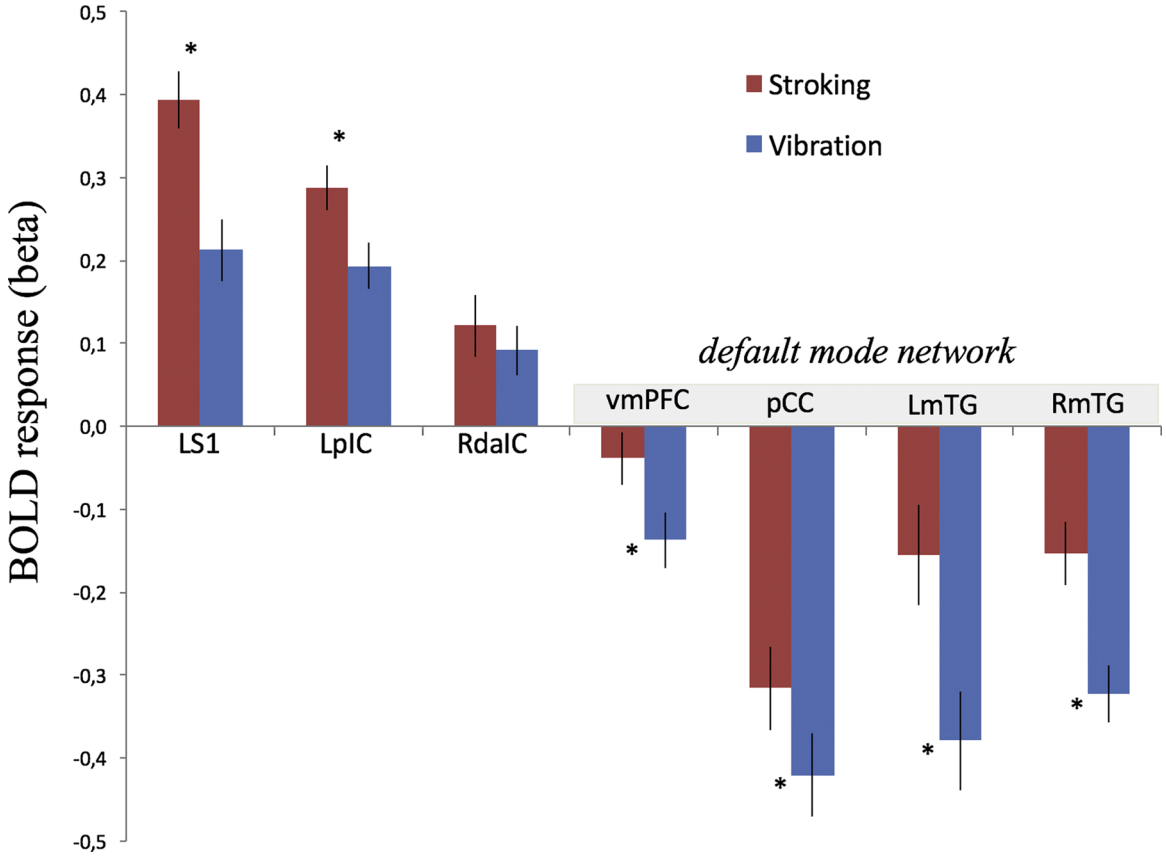

Fig. 5. Extracted beta values for stroking (red) and vibration (blue). Abbreviations: left S1 (LS1), left posterior insular cortex (LpIC), right dorsal anterior insula cortex (RdaIC), ventro medial prefrontal cortex (vmPFC), posterior cingulate cortex (pCC), left medial temporal gyrus (LmTG), right medial temporal gyrus (RmTG). Error bars correspond to SEM. * indicates two-sample-t-test p < .001.

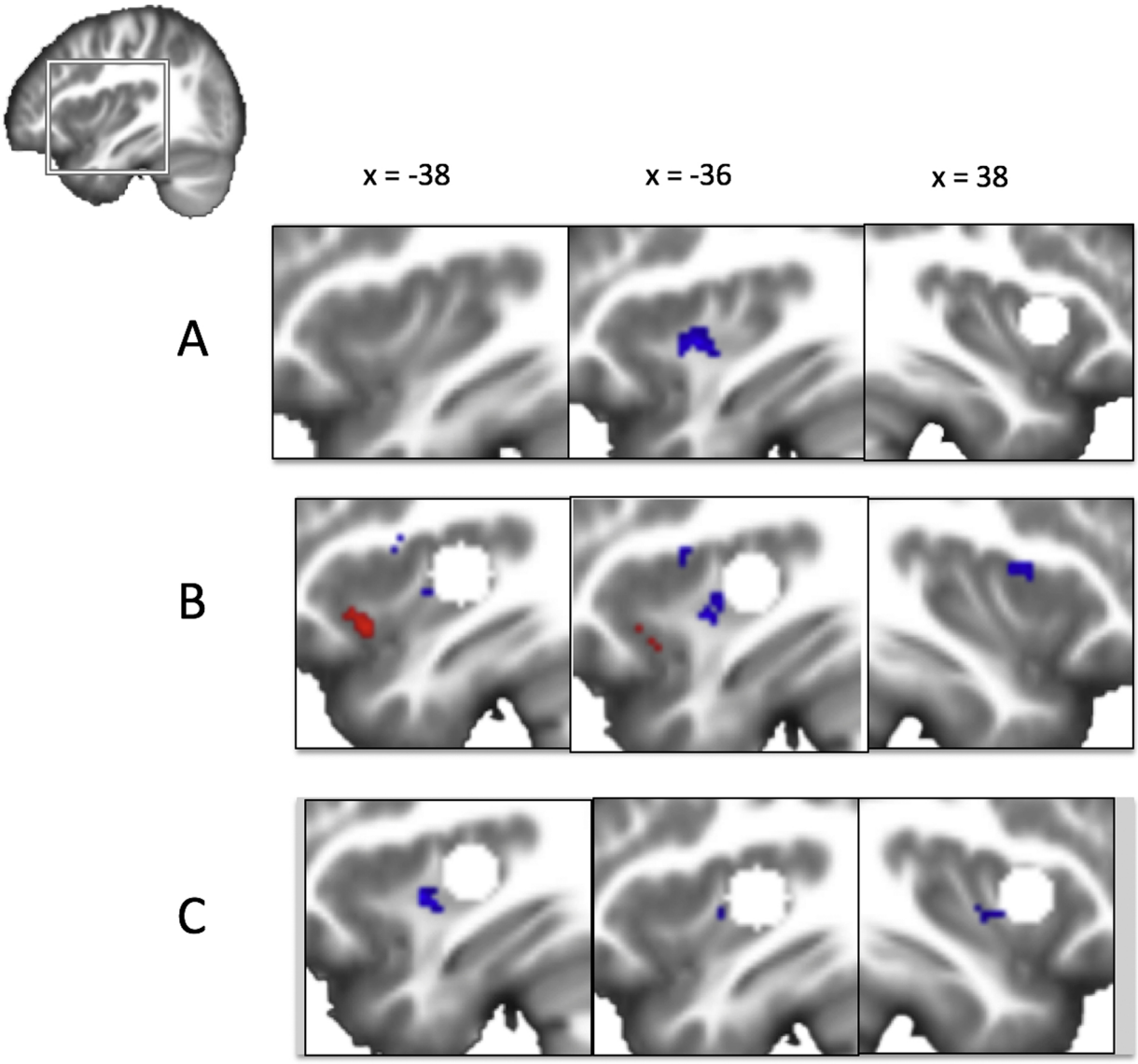

Fig. 6. Results from psychophysiological interaction analyses for seeds in A) right dorsal anterior insular cortex (RdaIC) and B) left posterior insular cortex (LpIC), masked with bilateral insular mask, and thresholded at $p < .005$ and cluster size > 18. C) Results from conjunction analysis RdaIC ∩ LpIC, masked with bilateral insular mask, and thresholded at $p < .001$ and cluster size > 9. Both contrasts stroking > vibration (red) and vibration > stroking (blue) are shown. White circles indicate seeds.

Table 2
Results from the psychophysiological interaction analyses for seeds in the right dorsal anterior insular cortex (RdaIC) and left posterior insular cortex (LpIC), and for the conjunction analysis RdaIC ∩ LPIC: t-values, MNI coordinates and cluster sizes (ks). t-value of 3.5 corresponds to p = .001. Positive t values correspond to contrast stroking > vibration, negative t values to vibration > stroking (thresholding as in Fig. 6).

Seed	Region in insula	t-value	x	y	z	ks
RdaIC	L Middle	−4,7	−36	0	−2	54
LPIC	L Ventral Anterior	3,5	−38	16	−12	21
	R Dorsal Anterior	−4,3	40	6	14	25
	L Middle	−3,9	−36	−2	−4	19
	L Dorsal Anterior	−3,7	−34	4	14	19
RdaIC ∩ LPIC	L Middle	−4,6	−36	0	−2	19
	R Middle	−4,5	36	2	−2	13

LpIC displayed an increase in functional connectivity with the left (contralateral to the site of stimulation) *vaIC* for stroking compared to vibration, and thus the stroking engaged processing in the emotional part of the insula.

Brain responses to the isolated CT activation have previously been studied in a patient (GL) who, at the age of 31, due to sensory ganglionopathy, lost functions mediated by Aβ afferents. However, her CT afferents are intact. In this patient, a task fMRI experiment in which slow skin stroking was applied on her right arm showed elevated BOLD responses in the left (contralateral to the stroking arm) posterior and left anterior insula, but no response in the *S1* or *S2* (Olausson et al., 2002). In our study we observed increased functional connectivity between the *LpIC* and *LvaIC* when we contrasted stroking versus vibration. Taken together these results suggest that the input from CT afferents is important for engaging affective insular processing of touch.

Another study investigated cortical thickness in GL, and showed that she displayed cortical thinning compared to the healthy subjects, in all areas except the right *aIC*, where the cortex was significantly thicker than in healthy subjects (Čeko et al., 2013). In the same study, resting state functional connectivity analysis on GL data revealed higher connectivity between the right *aIC* and bilateral *pIC*, and in addition between the insula and visual cortex, compared with the healthy subjects. The authors concluded that these results are the consequence of the plasticity changes in the insular cortex in patient GL, who uses isolated CT input together with the visual information as a compensation

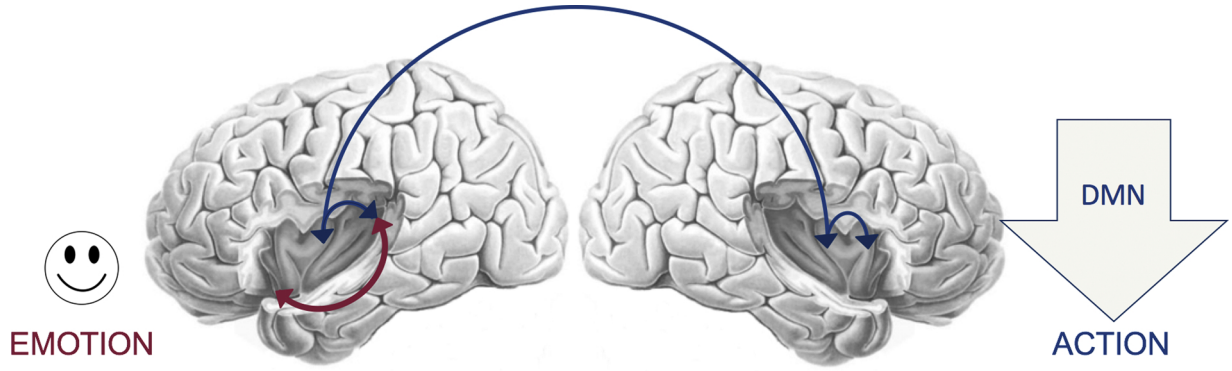

Fig. 7. Proposed mechanisms for processing of discriminative and emotional touch in insula. See text for explanation.

mechanism for her lack of discriminative touch, to navigate the environment. Our PPI analysis showed that the pathway between the *pIC* and *RdaIC* was indeed activated by discriminative touch (vibration) in healthy subjects. This analysis was, however, restricted to the bilateral insular cortex mask, and there are most certainly other brain regions involved in the processing of discriminative touch through the input from Aβ afferents in healthy subjects, that involve the *S1* and *S2* in particular. We thus speculate that, due to the loss of discriminative input from Aβ afferents, CTs in patient GL compensate to some extent this deficit by engaging the *pIC-RdaIC* discriminative pathway in insula to a higher extent than in healthy subjects.

A recent study investigated somatosensory responses in two patients with genetic mutation resulting in a loss of function of the PIEZO2 ion channel (Chesler et al., 2016). PIEZO2 is a mechanosensitive ion channel, expressed in the subset of somatosensory myelinated neurons. Sensory testing in these subjects showed a selective decrease in the discriminative touch perception, but a preserved response to the gentle skin stroking that typically activates CT afferents. An fMRI experiment in which gentle skin stroking was delivered to the left arm of one of the subjects, showed increased BOLD signal in the right *aIC* (contralateral to the stimulated arm), but no increase in the *S1* or *pIC*, confirming that preserved CT input is sufficient to activate the anterior insula.

4.1. Mechanism for processing of discriminative and emotional touch in the insula and neurodevelopmental aspects

The main conclusion from our analyses is that the insula processes affective touch information and also information about touch with less emotional valence, mainly conveyed via Aβ afferents. We suggest that pleasant (affective) touch is processed through interaction between the *pIC* and *vaIC* (Fig. 7). On the other hand, descriptive, less emotional, touch is processed through the interaction between the *pIC* and *RdaIC* via the middle insula. In the *RdaIC* the information reaches the SN, which in turn down-regulates the level of activity in the DMN depending on the cognitive demand of the sensory input.

The two pathways presented above have different neurodevelopmental trajectories. The development of *vaIC* follows a linear trajectory with monotonically decreasing cortical thickness from the early childhood, which is in agreement with the linear trend of pleasant experience of touch early in life (Croy et al., 2017). This continuous reduction may reflect experience dependent pruning and synaptic plasticity in this region (Brenhouse and Andersen, 2011). On the other hand, the descriptive pathway comprising *pIC* and *RdaIC* follows a more complex developmental process, with the increase in the cortical thickness during later childhood (with the peak at the age of 9) and decrease during adolescence (Shaw et al., 2008), which coincides with the critical period of functional specialization and cognitive development, determined by genetic factors and shaped through experience (Hensch, 2005). After the age of 10 both *vaIC* and *daIC* follow a linear path of cortical growth (Churchwell and Yurgelun-Todd, 2013). Based on these findings, it is tempting to hypothesize that the affective insular pathway has its critical period before the early childhood, and thus is vulnerable to the environmental damage already at birth (Rice and Barone, 2000).

4.2. Limitations

All analyses of task data in this study were performed on restricted ROIs and cluster level threshold was set to $p < .005$. Although this threshold might lead to the risk of type I error (Eklund et al., 2016), we note that the results show several consistencies. First, contrast stroking > vibration showed difference in all four areas central to the DMN. Secondly, PPI analysis for vibration > stroking showed overlapping areas in the bilateral middle insula, for seeds in the *LpIC* and *RdaIC*. Thus, our result might serve as guidance for future analyses of sensory processing in the insula.

Conflict of Interest

None.

References

Čeko, M., Seminowicz, D.A., Bushnell, M.C., Olausson, H.W., 2013. Anatomical and functional enhancements of the insula after loss of large primary somatosensory fibers. Cereb. Cortex 23, 2017–2024. http://dx.doi.org/10.1093/cercor/bhs157.

Ackerley, R., Wasling, H.B., Liljencrantz, J., Olausson, H., Johnson, R.D., Wessberg, J., 2014. Human C-tactile afferents are tuned to the temperature of a skin-Stroking caress. J. Neurosci. 34, 2879–2883. http://dx.doi.org/10.1523/JNEUROSCI.2847-13.2014.

Barnett, L., 2005. Keep in touch: the importance of touch in infant development. Infant Obs. 8, 115–123. http://dx.doi.org/10.1080/13698030500171530.

Björnsdotter, M., Löken, L., Olausson, H., Vallbo, Å., Wessberg, J., 2009. Somatotopic organization of gentle touch processing in the posterior insular cortex. J. Neurosci. 29, 9314–9320. http://dx.doi.org/10.1523/JNEUROSCI.0400-09.2009.

Brauer, J., Xiao, Y., Poulain, T., Friederici, A.D., Schirmer, A., 2016. Frequency of maternal touch predicts resting activity and connectivity of the developing social brain. Cereb. Cortex 26, 3544–3552. http://dx.doi.org/10.1093/cercor/bhw137.

Brenhouse, H.C., Andersen, S.L., 2011. Developmental trajectories during adolescence in males and females: a cross-species understanding of underlying brain changes. Neurosci. Biobehav. Rev. 35, 1687–1703. http://dx.doi.org/10.1016/j.neubiorev.2011.04.013.

Bystrova, K., 2009. Novel mechanism of human fetal growth regulation: a potential role of lanugo, vernix caseosa and a second tactile system of unmyelinated low-threshold C-afferents. Med. Hypotheses 72, 143–146. http://dx.doi.org/10.1016/j.mehy.2008.09.033.

Cascio, C.J., Lorenzi, J., Baranek, G.T., 2016. Self-reported pleasantness ratings and examiner-coded defensiveness in response to touch in children with ASD: effects of stimulus material and bodily location. J. Autism Dev. Disord. 46, 1528–1537. http://dx.doi.org/10.1007/s10803-013-1961-1.

Cascio, C.J., 2016. Psychiatric conditions and touch. Affect. Touch Neurophysiol. CT Afferents. Springer, New York, pp. 397–407. (accessed June 26, 2017). http://link.springer.com/chapter/10.1007/978-1-4939-6418-5_23.

Case, L.K., Laubacher, C.M., Olausson, H., Wang, B., Spagnolo, P.A., Bushnell, M.C., 2016. Encoding of touch intensity but not pleasantness in human primary somatosensory cortex. J. Neurosci. 36, 5850–5860. http://dx.doi.org/10.1523/JNEUROSCI.1130-15.2016.

Chesler, A.T., Szczot, M., Bharucha-Goebel, D., Čeko, M., Donkervoort, S., Laubacher, C., Hayes, L.H., Alter, K., Zampieri, C., Stanley, C., Innes, A.M., Mah, J.K., Grosmann,

C.M., Bradley, N., Nguyen, D., Foley, A.R., Le Pichon, C.E., Bönnemann, C.G., 2016. The role of PIEZO2 in human mechanosensation. N. Engl. J. Med. 0http://dx.doi.org/10.1056/NEJMoa1602812. (null).
Churchwell, J.C., Yurgelun-Todd, D.A., 2013. Age-related changes in insula cortical thickness and impulsivity: significance for emotional development and decision-making. Dev. Cogn. Neurosci. 6, 80–86. http://dx.doi.org/10.1016/j.dcn.2013.07.001.
Craig, A.D., 2002. How do you feel? Interoception: the sense of the physiological condition of the body. Nat. Rev. Neurosci. 3, 655–666. http://dx.doi.org/10.1038/nrn894.
Croy, I., Geide, H., Paulus, M., Weidner, K., Olausson, H., 2016. Affective touch awareness in mental health and disease relates to autistic traits −An explorative neurophysiological investigation. Psychiatry Res. 245, 491–496. http://dx.doi.org/10.1016/j.psychres.2016.09.011.
Croy, I., Sehlstedt, I., Wasling, H.B., Ackerley, R., Olausson, H., 2017. Gentle touch perception: from early childhood to adolescence. Dev. Cogn. Neurosci. http://dx.doi.org/10.1016/j.dcn.2017.07.009.
Davidovic, M., Jönsson, E.H., Olausson, H., Bjornsdotter, M., 2016. Posterior superior temporal sulcus responses predict perceived pleasantness of skin stroking. Front. Hum. Neurosci. 10, 432. http://dx.doi.org/10.3389/fnhum.2016.00432.
Deen, B., Pitskel, N.B., Pelphrey, K.A., 2011. Three systems of insular functional connectivity identified with cluster analysis. Cereb. Cortex 21, 1498–1506. http://dx.doi.org/10.1093/cercor/bhq186.
Dosenbach, N.U.F., Fair, D.A., Miezin, F.M., Cohen, A.L., Wenger, K.K., Dosenbach, R.A.T., Fox, M.D., Snyder, A.Z., Vincent, J.L., Raichle, M.E., Schlaggar, B.L., Petersen, S.E., 2007. Distinct brain networks for adaptive and stable task control in humans. Proc. Natl. Acad. Sci. 104, 11073–11078. http://dx.doi.org/10.1073/pnas.0704320104.
Eck, J., Kaas, A.L., Goebel, R., 2013. Crossmodal interactions of haptic and visual texture information in early sensory cortex. Neuroimage 75, 123–135. http://dx.doi.org/10.1016/j.neuroimage.2013.02.075.
Eklund, A., Nichols, T.E., Knutsson, H., 2016. Cluster failure: why fMRI inferences for spatial extent have inflated false-positive rates. Proc. Natl. Acad. Sci. 113, 7900–7905. http://dx.doi.org/10.1073/pnas.1602413113.
Fairhurst, M.T., Löken, L., Grossmann, T., 2014. Physiological and behavioral responses reveal 9-month-old infants' sensitivity to pleasant touch. Psychol. Sci. 25, 1124–1131. http://dx.doi.org/10.1177/0956797614527114.
Fox, M.D., Raichle, M.E., 2007. Spontaneous fluctuations in brain activity observed with functional magnetic resonance imaging. Nat. Rev. Neurosci. 8, 700–711. http://dx.doi.org/10.1038/nrn2201.
Friston, K.J., Price, C.J., Fletcher, P., Moore, C., Frackowiak, R.S.J., Dolan, R.J., 1996. The trouble with cognitive subtraction. Neuroimage 4, 97–104. http://dx.doi.org/10.1006/nimg.1996.0033.
Friston, K.J., Buechel, C., Fink, G.R., Morris, J., Rolls, E., Dolan, R.J., 1997. Psychophysiological and modulatory interactions in neuroimaging. Neuroimage 6, 218–229. http://dx.doi.org/10.1006/nimg.1997.0291.
Friston, K.J., Holmes, A.P., Price, C.J., Büchel, C., Worsley, K.J., 1999. Multisubject fMRI studies and conjunction analyses. Neuroimage 10, 385–396. http://dx.doi.org/10.1006/nimg.1999.0484.
Friston, K.J., Penny, W.D., Glaser, D.E., 2005. Conjunction revisited. Neuroimage 25, 661–667. http://dx.doi.org/10.1016/j.neuroimage.2005.01.013.
Grabenhorst, F., Rolls, E.T., 2011. Value, pleasure and choice in the ventral prefrontal cortex. Trends Cogn. Sci. 15, 56–67. http://dx.doi.org/10.1016/j.tics.2010.12.004.
Grabenhorst, F., D'Souza, A.A., Parris, B.A., Rolls, E.T., Passingham, R.E., 2010. A common neural scale for the subjective pleasantness of different primary rewards. Neuroimage 51, 1265–1274. http://dx.doi.org/10.1016/j.neuroimage.2010.03.043.
Grandi, L.C., Gerbella, M., 2016. Single neurons in the insular cortex of a macaque monkey respond to skin brushing: preliminary data of the possible representation of pleasant touch. Front. Behav. Neurosci. 10. http://dx.doi.org/10.3389/fnbeh.2016.00090.
Hensch, T.K., 2005. Critical period plasticity in local cortical circuits. Nat. Rev. Neurosci. 6. http://dx.doi.org/10.1038/nrn1787.
Kurth, F., Eickhoff, S.B., Schleicher, A., Hoemke, L., Zilles, K., Amunts, K., 2010a. Cytoarchitecture and probabilistic maps of the human posterior insular cortex. Cereb. Cortex 20, 1448–1461. http://dx.doi.org/10.1093/cercor/bhp208.
Kurth, F., Zilles, K., Fox, P.T., Laird, A.R., Eickhoff, S.B., 2010b. A link between the systems: functional differentiation and integration within the human insula revealed by meta-analysis. Brain Struct. Funct. 214, 519–534. http://dx.doi.org/10.1007/s00429-010-0255-z.
Löken, L.S., Wessberg, J., Morrison, I., McGlone, F., Olausson, H., 2009. Coding of pleasant touch by unmyelinated afferents in humans. Nat. Neurosci. 12, 547–548. http://dx.doi.org/10.1038/nn.2312.
Lindgren, L., Westling, G., Brulin, C., Lehtipalo, S., Andersson, M., Nyberg, L., 2012. Pleasant human touch is represented in pregenual anterior cingulate cortex. Neuroimage 59, 3427–3432. http://dx.doi.org/10.1016/j.neuroimage.2011.11.013.
McGlone, F., Wessberg, J., Olausson, H., 2014. Discriminative and affective touch: sensing and feeling. Neuron 82, 737–755. http://dx.doi.org/10.1016/j.neuron.2014.05.001.
Mesulam, M.-M., Mufson, E.J., 1982. Insula of the old world monkey. Architectonics in the insulo-orbito-temporal component of the paralimbic brain. J. Comp. Neurol. 212, 1–22. http://dx.doi.org/10.1002/cne.902120102.
Morel, A., Gallay, M.N., Baechler, A., Wyss, M., Gallay, D.S., 2013. The human insula: architectonic organization and postmortem MRI registration. Neuroscience 236, 117–135. http://dx.doi.org/10.1016/j.neuroscience.2012.12.076.
Morrison, I., Löken, L.S., Olausson, H., 2009. The skin as a social organ. Exp. Brain Res. 204, 305–314. http://dx.doi.org/10.1007/s00221-009-2007-y.
Morrison, I., Björnsdotter, M., Olausson, H., 2011a. Vicarious responses to social touch in posterior insular cortex are tuned to pleasant caressing speeds. J. Neurosci. 31, 9554–9562. http://dx.doi.org/10.1523/JNEUROSCI.0397-11.2011.
Morrison, I., Löken, L.S., Minde, J., Wessberg, J., Perini, I., Nennesmo, I., Olausson, H., 2011b. Reduced C-afferent fibre density affects perceived pleasantness and empathy for touch. Brain 134, 1116–1126. http://dx.doi.org/10.1093/brain/awr011.
Olausson, H., Lamarre, Y., Backlund, H., Morin, C., Wallin, B.G., Starck, G., Ekholm, S., Strigo, I., Worsley, K., Vallbo, Å.B., Bushnell, M.C., 2002. Unmyelinated tactile afferents signal touch and project to insular cortex. Nat. Neurosci. 5, 900–904. http://dx.doi.org/10.1038/nn896.
Olausson, H.W., Cole, J., Vallbo, Å., McGlone, F., Elam, M., Krämer, H.H., Rylander, K., Wessberg, J., Bushnell, M.C., 2008. Unmyelinated tactile afferents have opposite effects on insular and somatosensory cortical processing. Neurosci. Lett. 436, 128–132. http://dx.doi.org/10.1016/j.neulet.2008.03.015.
Olausson, H., Wessberg, J., Morrison, I., McGlone, F., Vallbo, Å., 2010. The neurophysiology of unmyelinated tactile afferents. Neurosci. Biobehav. Rev. 34, 185–191. http://dx.doi.org/10.1016/j.neubiorev.2008.09.011.
Panchuelo, R.M.S., Ackerley, R., Glover, P.M., Bowtell, R.W., Wessberg, J., Francis, S.T., McGlone, F., 2016. Mapping quantal touch using 7 Tesla functional magnetic resonance imaging and single-unit intraneural microstimulation. eLife 5, e12812. http://dx.doi.org/10.7554/eLife.12812.
Perini, I., Olausson, H., Morrison, I., 2015. Seeking pleasant touch: neural correlates of behavioral preferences for skin stroking. Front. Behav. Neurosci. 9. http://dx.doi.org/10.3389/fnbeh.2015.00008.
Raichle, M.E., 2015. The brain's default mode network. Annu. Rev. Neurosci. 38, 433–447. http://dx.doi.org/10.1146/annurev-neuro-071013-014030.
Rice, D., Barone, S., 2000. Critical periods of vulnerability for the developing nervous system: evidence from humans and animal models. Environ. Health Perspect. 108, 511–533.
Sehlstedt, I., Ignell, H., Backlund Wasling, H., Ackerley, R., Olausson, H., Croy, I., 2016. Gentle touch perception across the lifespan. Psychol. Aging 31, 176–184. http://dx.doi.org/10.1037/pag0000074.
Shaw, P., Kabani, N.J., Lerch, J.P., Eckstrand, K., Lenroot, R., Gogtay, N., Greenstein, D., Clasen, L., Evans, A., Rapoport, J.L., Giedd, J.N., Wise, S.P., 2008. Neurodevelopmental trajectories of the human cerebral cortex. J. Neurosci. 28, 3586–3594. http://dx.doi.org/10.1523/JNEUROSCI.5309-07.2008.
Song, X.-W., Dong, Z.-Y., Long, X.-Y., Li, S.-F., Zuo, X.-N., Zhu, C.-Z., He, Y., Yan, C.-G., Zang, Y.-F., 2011. REST. a toolkit for resting-state functional magnetic resonance imaging data processing. PLoS One 6, e25031. http://dx.doi.org/10.1371/journal.pone.0025031.
Stack, D.M., Muir, D.W., 1992. Adult tactile stimulation during face-to-face interactions modulates five-month-olds' affect and attention. Child Dev. 63, 1509–1525. http://dx.doi.org/10.1111/j.1467-8624.1992.tb01711.x.
Uddin, L.Q., Kinnison, J., Pessoa, L., Anderson, M.L., 2014. Beyond the tripartite cognition-emotion-interoception model of the human insular cortex. J. Cogn. Neurosci. 26, 16–27. http://dx.doi.org/10.1162/jocn_a_00462.
Uddin, L.Q., 2015. Salience processing and insular cortical function and dysfunction. Nat. Rev. Neurosci. 16, 55–61. http://dx.doi.org/10.1038/nrn3857.
Whitfield-Gabrieli, S., Nieto-Castanon, A., 2012. Conn a functional connectivity toolbox for correlated and anticorrelated brain networks. Brain Connect. 2, 125–141. http://dx.doi.org/10.1089/brain.2012.0073.